ORP2, a homolog of oxysterol binding protein, regulates cellular cholesterol metabolism

Saara Laitinen,* Markku Lehto,* Sanna Lehtonen,† Kati Hyvärinen,* Sanna Heino,* Eero Lehtonen,† Christian Ehnholm,* Elina Ikonen,* and Vesa M. Olkkonen[1,*]

Department of Molecular Medicine,* National Public Health Institute, Biomedicum, P.O. Box 104, FIN-00251 Helsinki, Finland; and Department of Pathology,† Haartman-Institute, P.O. Box 21, FIN-00014, University of Helsinki, Finland

Abstract Oxysterol binding protein (OSBP) related proteins (ORPs) constitute a family that has at least 12 members in humans. In the present study we characterize one of the novel OSBP homologs, ORP2, which we show to be expressed ubiquitously in mammalian tissues. The ORP2 cDNA encodes a deduced 55 kDa protein that lacks a pleckstrin homology (PH) domain, a feature found in the other family members. Sucrose gradient centrifugation analysis of Chinese hamster ovary (CHO) cell post-nuclear supernatant demonstrated that ORP2 is distributed in soluble and membrane-bound fractions. Immunofluorescence microscopy of the endogenous and overexpressed ORP2 in CHO cells suggested that the membrane-bound fraction of the protein localizes to the Golgi apparatus. Stably transfected CHO cells that overexpress ORP2 showed an increase in [^{14}C]cholesterol efflux to serum, apolipoprotein A-I (apoA-I), and phosphatidyl choline vesicles. The proportion of cellular [^{14}C]cholesterol that is esterified and the ACAT activity measured as [^{14}C]oleyl-CoA conversion into cholesteryl [^{14}C]oleate by the cellular membranes, were markedly decreased in the ORP2 expressing cells. Transient high level overexpression of ORP2 interfered with the clearance of a secretory pathway protein marker from the Golgi complex. The results implicate ORP2 as a novel regulator of cellular sterol homeostasis and intracellular membrane trafficking.—Laitinen, S., M. Lehto, S. Lehtonen, K. Hyvärinen, S. Heino, E. Lehtonen, C. Ehnholm, E. Ikonen, and V. M. Olkkonen. **ORP2, a homolog of oxysterol binding protein, regulates cellular cholesterol metabolism. *J. Lipid Res.* 2002.** 43: **245–255.**

Supplementary key words cholesterol efflux • cholesterol esterification • Golgi apparatus • mRNA expression • protein expression • membrane trafficking

Oxysterols are 27-carbon products of cholesterol oxidation that participate in different aspects of lipid metabolism. They are regulators of gene expression, substrates for bile acid synthesis, and mediators of sterol transport (1, 2). Furthermore, they are suggested to be involved in the development of atherosclerosis (3). The regulatory effects of oxysterols on lipid metabolism have been attributed to oxysterol-binding members of the orphan nuclear receptor superfamily. The liver X receptors, upon binding of oxysterol ligands, regulate the transcription of several genes important for the maintenance of the body cholesterol homeostasis. In addition, oxysterols control the biosynthesis of steroid hormones and the development of steroidogenic tissues through regulation of the activity of steroidogenic factor-1 (4, 5)

The oxysterol binding protein (OSBP) was the first protein shown to interact with oxysterols, and it was anticipated to be involved in the control of sterol regulated gene expression (6, 7). OSBP does not belong to the superfamily of nuclear receptors; it is a cytosolic protein that upon ligand binding translocates to Golgi membranes (8). This membrane interaction depends on a pleckstrin homology (PH) domain in the *N*-terminal part of the protein (8–10). Even though OSBP was not found to be a major controller of transcription of the genes responsible for cellular cholesterol homeostasis (11), several studies have shown that OSBP does play a role in the regulation of cellular cholesterol and sphingomyelin biosynthesis (9, 12). These findings support a role of OSBP in the maintenance of the cellular lipid balance, but the mechanisms by which OSBP causes such effects are poorly understood. The genome of the yeast *Saccharomyces cerevisiae* encodes seven OSBP homologs, which are suggested to constitute an essential regulatory device involved in yeast sterol metabolism (13). Interestingly, one of the yeast OSBP homologs,

Abbreviations: ABCA1, ATP-binding cassette transporter A1; apoA-I, apolipoprotein A-I; CE, cholesteryl ester; CHO, Chinese hamster ovary cells; ECL, enhanced chemiluminescence; ER, endoplasmic reticulum; FC, free cholesterol; GFP, green fluorescent protein; GST, glutathione-S-transferase; MTE, multiple tissue expression; IMDM, Iscove's Modified Dulbecco's Medium; OHC, hydroxycholesterol; ORP, oxysterol binding protein related protein; OSBP, oxysterol binding protein; PA, phosphatidic acid; PFA, paraformaldehyde; PH, pleckstrin homology; POPC, 1-palmitoyl-2-oleyl-phosphatidylcholine; SUV, small unilamellar vesicles; TC, total cholesterol; VSVG, vesicular stomatitis virus G protein.

[1] To whom correspondence should be addressed.
e-mail: vesa.olkkonen@ktl.fi

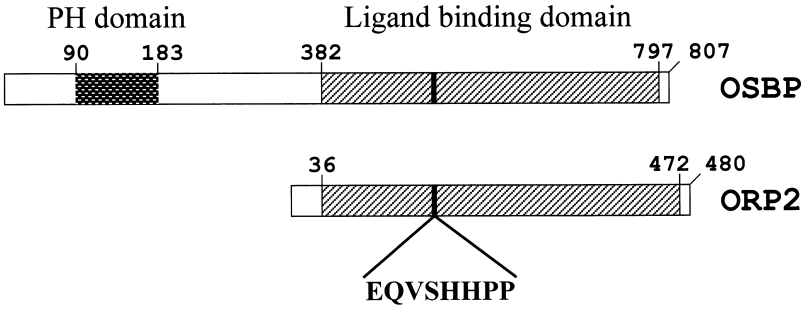

Fig. 1. Alignment of the oxysterol binding protein related protein two (ORP2) and oxysterol binding protein (OSBP) protein sequences. The sequences are aligned according to a highly conserved sequence motif, the "OSBP fingerprint," EQVSHHPP. The numbers above the bars indicate amino acid positions.

Kes1p/Osh4p, has also been implicated in the biogenesis of secretory vesicles at the Golgi apparatus (14).

We have recently identified a family of human OSBP related proteins (ORP) (15, 16). In the present study we characterize one of the family members, ORP2. The full-length ORP2 cDNA encodes a deduced 480 amino acid residue protein with a predicted molecular mass of 55 kDa (16). The protein shows significant homology to the sterol binding domain of OSBP (**Fig. 1**). The amino acid identity between ORP2 and OSBP in this region is 39%. ORP2 lacks the *N*-terminal extension present in OSBP that contains a pleckstrin homology (PH) domain required for the Golgi localization and the functional effects of OSBP (9, 10, 17). In the present study we report the expression patterns of ORP2 mRNA and protein, as well as the intracellular localization and some functional effects of the protein.

MATERIALS AND METHODS

Materials. [^{3}H]cholesterol (49.0 Ci/mmol) and [^{14}C]cholesterol (54.0 mCi/mmol) were purchased from Amersham (Piscataway, NJ), and different [^{3}H]oxysterols were kindly provided by Prof. Ingemar Björkhem (Karolinska Institute, Huddinge, Sweden). Geneticin (G-418 sulfate) was from Life Technologies (Rockville, MD), 1-palmitoyl-2-oleyl-phosphatidylcholine (POPC) from Avanti Polar Lipids (Alabaster, AL), [1-^{14}C]oleyl-CoA (56 mCi/mmol) from Amersham, and FITC-lentil lectin from Molecular Probes (Eugene, OR).

Cell culture. COS-1 cells were cultured in DMEM (Sigma, St. Louis, MO), 10% FBS, 100 IU/ml penicillin, 100 μg/ml streptomycin, and Chinese hamster ovary (CHO)-K1 cells in Iscove's Modified Dulbecco's Medium (IMDM, Sigma), 10% FBS, 100 IU/ml penicillin, 100 μg/ml streptomycin.

cDNA constructs. The ORP2 cDNA (KIAA0772, acc no AB018315) obtained from Dr. T. Nagase (Kazusa DNA Research Institute, Chiba, Japan) (18) was inserted into the *Bam*HI site of pGAT-4 vector (Dr. J. Peränen, Institute of Biotechnology, Helsinki, Finland), and the construct was used for protein production in *Escherichia coli*. For mammalian cell expression, the sequence was corrected to include the missing 36 nucleotides (16) (acc. nos AK000230 and AF331963) by a PCR approach. The full-length cDNA was then subcloned into the EcoRV-XhoI sites of pcDNA3.1(+) (Invitrogen). All constructs were verified by sequencing with a cycle-sequencing kit (Bigdye, Applied Biosystems, Foster City, CA) and an automated ABI377 sequencer (Applied Biosystems).

Determination of the ORP2 mRNA tissue expression pattern. The full-length ORP2 was excised from the pcDNA3.1(+) vector and labeled by random priming using [^{32}P]dATP (Amersham), random hexamer primers (Promega, Madison, WI), and the Klenow enzyme (New England Biolabs, Beverly, MA). Hybridization of a human Multiple Tissue Expression (MTE) filter array (Clontech, Palo Alto, CA) was carried out according to the manufacturer's instructions. The hybridization signals were quantified using the Fuji BAS1500 imaging system.

In situ hybridization. In situ hybridization was performed essentially as described (19). A mouse ORP2 cDNA probe was isolated by RT-PCR from mouse brain total RNA using the following primers: TCGCGGATCCAACTCTGCTCAGATGTATA (5′-primer) and TCCGGAATTCAAAGTAATGGCCGGCGTAC (3′-primer). pBluescript SK(−) carrying the isolated cDNA fragment was linearized either with *Bam*HI or *Eco*RI for the production of antisense or sense probes, respectively. The single-stranded RNA probes were labeled with [^{35}S]- UTP_S (Amersham) by the T3/T7 run off-transcription method (Riboprobe II Core System, Promega). Embryonic day-12 whole embryos were fixed with 4% paraformaldehyde (PFA) and embedded in paraffin. Five-micrometer sections were hybridized at 52°C for 15–20 h, with antisense and sense probes in parallel, in 60% deionized formamide, 0.3 M NaCl, 20 mM Tris-HCl (pH 8.0), 5 mM EDTA, pH 8.0, 10% dextran sulfate (Mw 500,000), 1× Denhardt's solution, 0.5 mg/ml torula yeast RNA, and 0.1 M dithiothreitol (DTT). After hybridization the sections were washed in high stringency conditions [including a wash twice at 65°C for 30 min in 50% deionized formamide, 2× SSC (0.3 M NaCl, 0.03 M Na-citrate, pH 7.0), 30 mM DTT], dipped in Kodak NTB-2 autoradiography emulsion and exposed at 4°C for 4 weeks.

Antibodies. A glutathione-*S*-transferase (GST)-ORP2 fusion protein was expressed under standard conditions in *E. coli* BL21 (DE3) and purified from inclusion bodies by preparative 12.5% acrylamide SDS-PAGE. The protein was used for immunization of HsdRIVM: ELCO rabbits. For affinity purification of the antibodies, the fusion protein was expressed at room temperature to make it soluble, purified, and covalently attached to cyanogen bromide activated Sepharose 4B (Pharmacia, Peapack, NJ). For affinity purification of anti-ORP2 antibodies the antiserum, diluted 1:5 with PBS, was first incubated for 2 h at room temperature with a Sepharose 4B column containing covalently coupled GST. Thereafter the unbound fraction was incubated with GST-ORP2-Sepharose at 4°C overnight. The antibodies were eluted with 200 mM glycine, pH 2.8, neutralized, and dialyzed against PBS.

Western blotting. Proteins were separated in 12.5% SDS-acrylamide gels and transferred to Hybond-C nitrocellulose (Amersham) according to the manufacturer's instructions. Nonspecific binding of antibodies was blocked with 5% fat-free cow's milk in 10 mM Tris/HCl, pH 7.4, 150 M NaCl, 0.1% Tween-20. The bound antibodies were visualized with horseradish-peroxidase-conjugated goat anti-rabbit IgG (Bio-Rad, Hercules, CA) and the enhanced-chemiluminescence system (ECL, Amersham).

Tranfections and selection of stably transfected CHO cells. CHO-K1 cells were transfected for transient overexpression with pcDNA 3.1 (+)/ORP2, the VSVG3-green fluorescent protein (GFP) expression plasmid (20) or control plasmids using Lipofectamine

2000 (Life Technologies). Selection of CHO-K1 cells stably transfected with the pcDNA 3.1 (+)/ORP2 or the plain vector plasmid was performed according to the Invitrogen protocol using Lipofectamine 2000, and 400 μg/ml of Geneticin (G-418 sulfate) in the growth medium. Cells overexpressing ORP2 were identified by immunofluorescence microscopy with rabbit anti-ORP2 antibodies, and single cell cloning was carried out by limiting dilution. All transfections were done according to the manufacturers' instructions.

Flotation of cellular membranes in sucrose gradients. CHO-K1 cells were grown on 6 cm plastic dishes. After PBS washes the cells were scraped in 250 mM sucrose, 140 mM KCl, 10 mM HEPES, pH 7.4, and broken by repeated passages through a 21 G needle. After removal of nuclei and intact cells, sucrose was added to a final concentration of 2 M (total volume of 2.5 ml). This was overlayed with 2 ml of 1.7 M of sucrose, 1 ml 0.8 M sucrose, 140 mM KCl, and 10 mM HEPES. The gradients were centrifuged at 130,000 *g* in a SW50.1 rotor at 10°C for 17 h. Fractions of 1 ml were collected from the top, and the proteins were chloroform-methanol precipitated and analyzed by SDS-PAGE and Western blotting.

Immunofluorescence microscopy. CHO-K1 cells were fixed with 4% paraformaldehyde, 250 mM Hepes, pH 7.4 for 30 min. Cells were then permeabilised with 0.1% Triton X-100 in PBS for 20 min, and unspecific binding of antibodies was blocked with 10% FBS/PBS for 30 min. The cells were then incubated with affinity purified ORP2 antibody at 4°C overnight, and with rhodamine-conjugated goat anti-rabbit IgG $F(ab)_2$ (Immunotech) at 37°C for 1 h. The specimens were mounted in Mowiol (Calbiochem, La Jolla, CA) containing 50 mg/ml of 1,4-diazabicyclo-[2.2.2]octane (Sigma). To test the specificity of the antibody, it was (before application to cell specimens) pre-incubated with purified GST or GST-ORP2 protein (at 50 μg/ml) at room temperature for 3 h. The specimens were analyzed using a Leica TCS SP laser scanning confocal microscope system.

Analysis of cholesterol efflux and esterification. One day before the experiments, stably transfected ORP2/CHO or mock-transfected CHO cells were seeded on 3 cm dishes and cultured in IMDM containing 10% FBS, 100 IU/ml of penicillin, 100 μg/ml streptomycin, and 400 μg/ml G-418. [^{14}C]cholesterol (54 μCi/mmol) was added in fresh serum containing medium (0.2 μCi per dish in a volume of 2 ml), followed by a 36 h incubation at 37°C. Cholesterol efflux was performed either to 20% human serum in IMDM medium, to 0.2% defatted BSA/IMDM medium in the presence or absence of 20 μg/ml of Swiss apoA-I (kindly provided by Dr. Peter Lerch, Swiss Red Cross), or to IMDM medium containing small unilamellar vesicles [0.3 mg phosphatidylcholine (PC)/ml] prepared from POPC (see below). The growth medium was discarded, the cells were washed twice with PBS, and 1 ml of medium containing the efflux acceptor was added per dish. After 2 h (serum acceptor) or 4 h (apoA-I or PC vesicle acceptors) at 37°C, the media were harvested and centrifuged, and the radioactivity in the supernatant was measured. The cells were scraped in 1 ml of ice-cold 2% NaCl and combined with the pellet obtained from the centrifuged media. The cells were vortexed and 100 μl were taken for radioactivity measurements by scintillation counting. Esterification of the [^{14}C]cholesterol was analyzed from labeled cell aliquots harvested before initiation of the efflux reactions, according to (21, 22).

Preparation of PC vesicles. Small unilamellar vesicles (SUV) were prepared by sonication of POPC in 0.15 M KCl buffer for 30 min in 5 min bursts (5 μm amplitude), and 2 min cooling periods using a Sanyo Soniprep 150 sonicator. After sonication, multilamellar vesicles and undispersed lipids were removed by centrifugation at 55,000 rpm, 4°C, for 2 h in a Beckmann TL 100.1 rotor (23). The supernatant was stored under N_2 at 4°C and used within 1 week. The phospholipid content was measured colorimetrically using Phospholipids B kit of Wako Chemicals GmbH (Neuss, Germany).

Determination of ACAT activity. The ACAT activity of mock- or ORP2-transfected stable CHO-K1 lines cultured in IMDM, 10% FBS, and G-418 (400 μg/ml) was determined as [^{14}C]oleyl-CoA

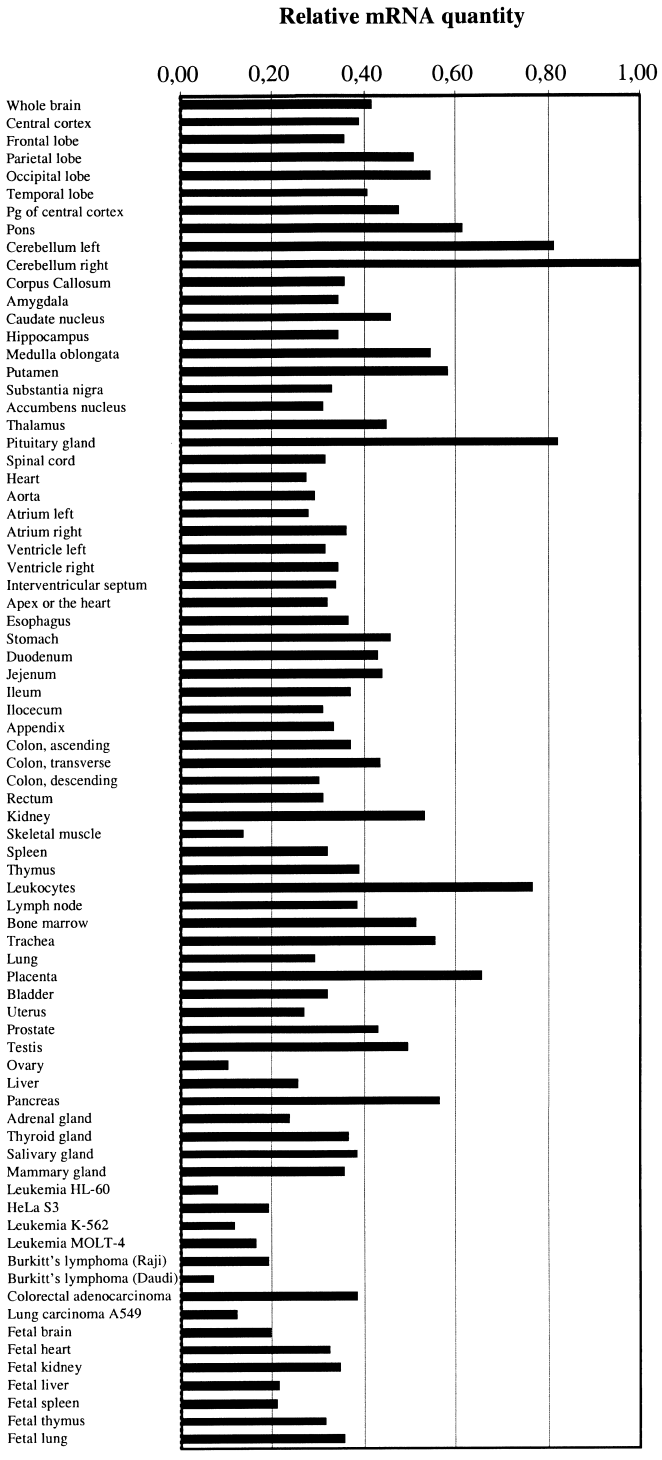

Fig. 2. Expression of ORP2 mRNA in human tissues and cell lines. A multiple tissue expression (MTE) filter array (Clontech) was hybridized with a [^{32}P]dATP labeled full-length ORP2 cDNA probe, and the signals were quantified using the Fuji BAS1500 imaging system. The expression levels are shown on a relative scale; the highest signal was designated 1. The mRNA source tissues and cell lines are indicated.

incorporation into cholesterol ester (CE) by semipurified cellular membranes according to Metherall et al (24). Measurements were carried out in the presence of exogenously added cholesterol (20 μg/ml final concentration).

Analysis of the cellular cholesterol content. In order to analyze total, free, and esterified cholesterol in the stably transfected cell lines, cells grown on 3 cm dishes were homogenized in 1 ml of 2% NaCl. [^{14}C]cholesterol was added to the homogenate to be able to correct the results for material losses. Aliquots of 100 μl were taken to protein analysis and radioactivity measurement. From the remaining 800 μl, lipids were extracted with 1:1 chloroform-methanol according to Bligh et al. (21) and Heino et al. (22); the lower phase containing the lipids was evaporated under nitrogen, lyophilized for 1 h, and dissolved in 120 μl methanol. The cholesterol amounts were measured enzymatically using either Cholesterol CHOD-PAP (Kit 1489232, Roche) for total cholesterol or Free Cholesterol C (Kit 274-47109E, Wako) for free cholesterol. Esterified cholesterol was calculated by subtracting the free cholesterol from the total cholesterol. Protein amounts were measured using DC Protein Assay (Bio-Rad). All cholesterol amounts were calculated as μg of cholesterol/mg of protein.

Analysis of marker protein trafficking through the secretory pathway. CHO-K1 cells were seeded on coverslips one day before transfection, and transfected with the VSVG3-GFP expression plasmid encoding a GFP-tagged form of vesicular stomatitis virus G protein ts045 mutant (20), together with either pcDNA 3.1 (+)/ORP2 or

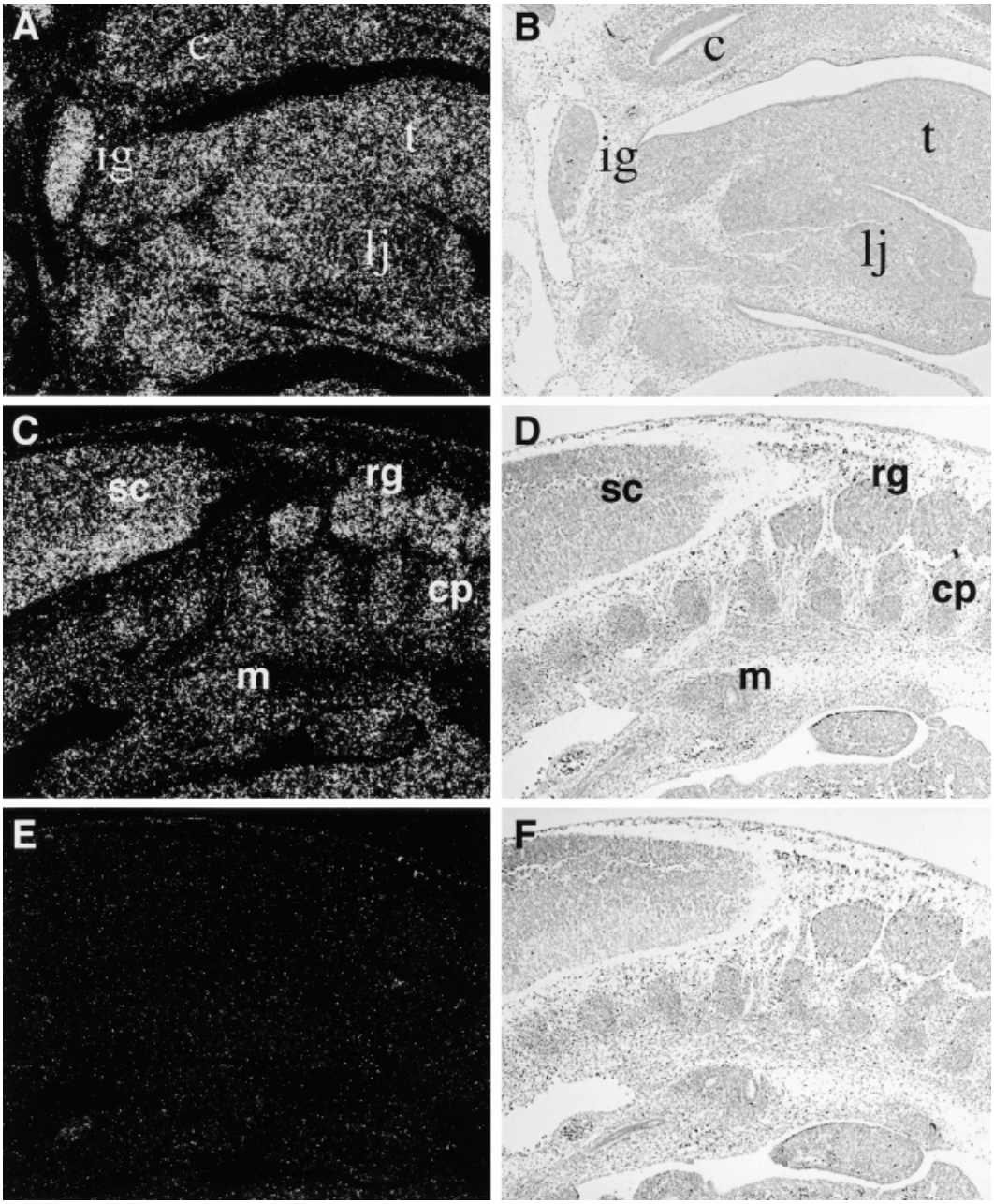

Fig. 3. Expression of ORP2 mRNA in mouse embryonic tissues. Sections of 12-day mouse embryos were hybridized with [^{35}S]UTP_S-labeled mouse ORP2 riboprobes of antisense (A–D) or sense polarity (E–F). A, C, and E are darkfield, and B, D, and F brightfield images. The structures/tissues indicated by lettering are A, B: c, cochlea; ig, inferior ganglion of vagus nerve; t, tongue; lj, lower jaw; C, D: sc, spinal cord; rg, dorsal root ganglia; m, metanephric kidney; cp, cartilage primordium.

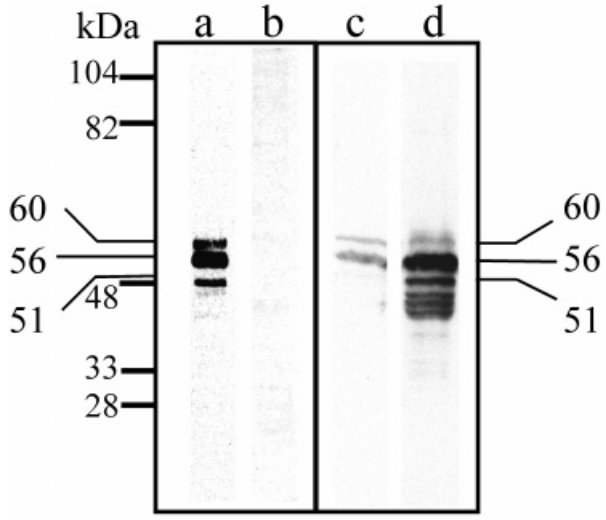

Fig. 4. Western blot analysis of the ORP2 protein in CHO cells. Cell lysates were resolved by SDS-PAGE, transferred onto nitrocellulose, and stained with affinity-purified rabbit antibodies against ORP2. The bound antibodies were visualized using HRP-conjugated anti-rabbit IgG and enhanced chemiluminescence (ECL). Lane a: the antibody was preincubated with GST; Lane b: the antibody was preincubated with GST-ORP2; Lanes c, d: untransfected CHO cells and cells transiently transfected with full-length ORP2 cDNA, respectively. The staining in c is weaker than in a, due to a shorter exposure time used to avoid overexposure of lane d. Mobilites of molecular weight markers, as well as the apparent molecular masses of the major ORP2 isoforms detected, are indicated.

pcDNA 3.1/CAT as a control plasmid, using Lipofectamine 2000 (Life Technologies). After 4 h of transfection at 37°C, the cells were transferred to 40°C for 16 h. The cells were then shifted to 32°C in HEPES-buffered medium containing cycloheximide (50 μg/ml). The cells were fixed at different time points with paraformaldehyde (see above) and processed for fluorescence microscopy with a Leica TCS SP confocal microscope.

RESULTS

We have previously reported that the ORP2 mRNA is expressed in most human tissues, and that several mRNA sizes can be observed (15). We now describe in more detail the tissue-specific expression pattern of ORP2 mRNA using a MTE filter array (Clontech) that contains mRNA from 76 human tissues and cell lines. ORP2 mRNA was detected in all tissues/cell lines studied (**Fig. 2**). Phosphorimager quantitation of the hybridized probe revealed that highest mRNA levels were present in specific parts of the central nervous system (cerebellum, pituitary gland, pons, and putamen) as well as in leukocytes, placenta, and pancreas. The difference between the weakest (ovary) and the strongest (cerebellum right) tissue signals was approximately 10-fold. To find out whether the expression of ORP2 mRNA in mammalian tissues is concentrated in specific cell types, in situ hybridization was carried out on sections prepared from day-12 mouse embryos. Also in this analysis, the mRNA showed ubiquitous and considerably even distribution both between and within different tissues (**Fig. 3**). Certain tissues, however, could be distinguished as ones displaying more prominent expression. These included parts of the developing central and peripheral nervous system: the spinal cord, the dorsal root ganglia (Fig. 3C), and the inferior ganglion of the vagus nerve (Fig. 3A). The corresponding sense riboprobe yielded a low and uniform background (Fig. 3E), demonstrating the specificity of the signals observed.

To monitor the distribution of the ORP2 protein, a rabbit antibody generated against a GST-ORP2 fusion protein expressed in *E. coli* was used. The antibody was (after preadsorption on a matrix with covalently bound GST) affinity purified using a GST-ORP2 matrix. In Western blots of CHO cell lysates (**Fig. 4**, lane a), this antibody detected a major endogenous protein band of 56

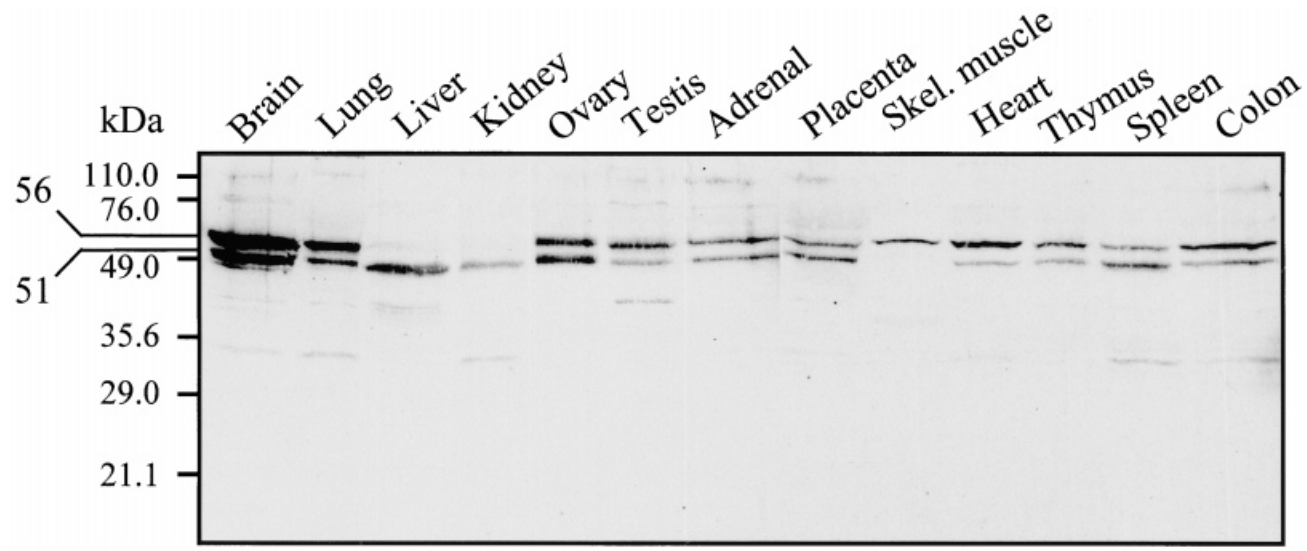

Fig. 5. Western blot analysis of ORP2 in mouse tissues. Tissues homogenates (15 μg protein from each tissue) were analyzed as described in the legend for Fig. 4. The tissues are identified on the top. Mobilites of molecular weight markers, as well as the apparent molecular masses of the major ORP2 isoforms, are indicated on the left.

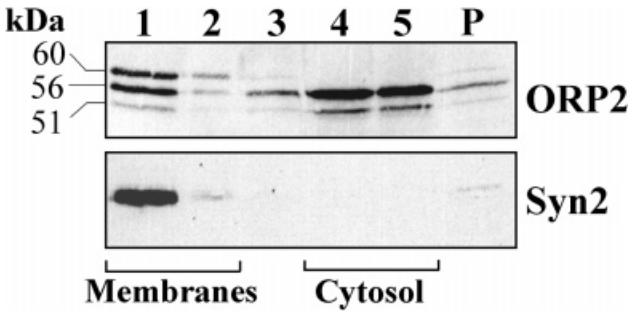

Fig. 6. Distribution of ORP2 between cellular membranes and cytosol. CHO cells were homogenized and the post-nuclear supernatant was analyzed by ultracentrifugation in sucrose gradients. Fractions were collected from the top of the gradients; P = pellet. The top panel: fractions analyzed by SDS-PAGE and Western blotting using the affinity-purified antibody against ORP2. The apparent molecular masses of the major ORP2 isoforms are indicated on the left. The bottom panel: fractions analyzed for syntaxin 2 (Syn2), an integral membrane protein used as a control.

kDa, and additional weaker bands with apparent molecular masses of 60 kDa and 51 kDa. Preincubation of the antibody with purified GST-ORP2 abolished the reactivity with all three protein bands (Fig. 4, lane b), suggesting that the reaction was specific for ORP2 and that the observed bands represent different forms of the protein. The 56 kDa protein coincided precisely with a strong protein band detected upon transient overexpression of the full-length cDNA in the cells (Fig. 4, lanes c, d). The apparent size of this protein band was in accordance with the size of ORP2 deduced from the cDNA sequence, 55 kDa. Upon overexpression of the cDNA, additional protein products apparently representing proteolytic fragments appeared in the 40–50 kDa size range. Western blot analysis of mouse tissue specimens revealed the presence of the ORP2 protein in all tissues studied (**Fig. 5**), with the highest protein expression in the brain. In most of the tissues, including the brain, the protein was present as two major bands with apparent molecular masses of 56

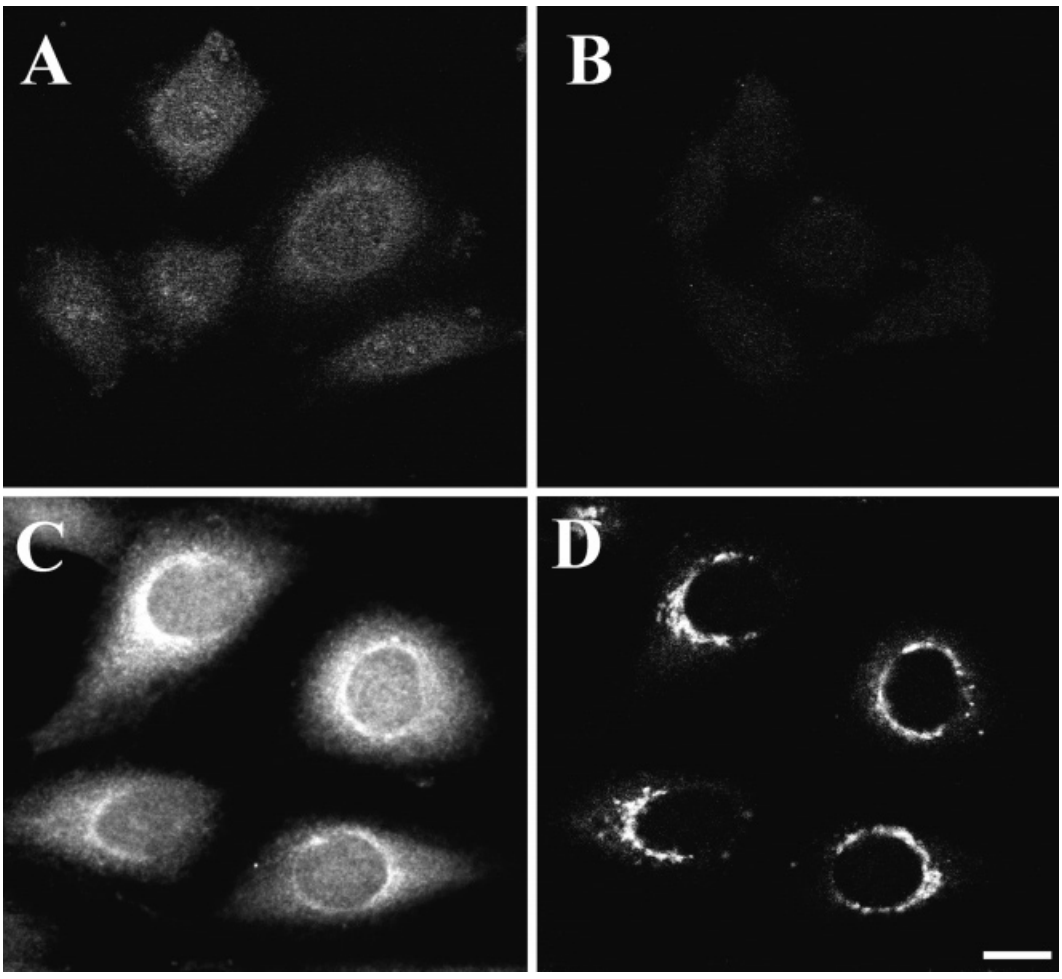

Fig. 7. Localization of ORP2 in CHO cells by indirect immunofluorescence microscopy. CHO cells were fixed with paraformaldehyde and processed for confocal immunofluorescence microscopy with affinity purified rabbit antibodies against ORP2 as described in Materials and Methods. A: Staining of endogenous ORP2 in CHO cells; the antibody was preincubated with purified GST. B: Specific reactivity was inhibited by preincubation of the antibody with GST-ORP2. The bottom panels, stably transfected CHO cells overexpressing ORP2 double stained with ORP2 antibodies (C) and with FITC-lentil lectin, a marker of the Golgi apparatus (D). Bar = 10 μm.

kDa and 51 kDa. In the mouse tissues the 60 kDa form seen in CHO cells was not observed. In mouse liver and kidney, only the 51 kDa form was detected, whereas the 56 kDa was predominant in skeletal and heart muscle. Similar immunoreactive forms of the protein were also detected in human primary fibroblasts by Western blotting (not shown).

To determine the distribution of ORP2 between cytosol and cellular membranes, the post-nuclear supernatant of CHO cells was fractionated by ultracentrifugation in sucrose step gradients, followed by Western blotting of the fractions (**Fig. 6**). Syntaxin 2, an integral membrane protein used as a control, was quantitatively found in the floating top fractions. The 56 kDa and the 51 kDa forms distributed between the membranes (~20%) and the bottom fractions containing soluble proteins (~80%), while the 60 kDa form not detected in mouse tissues was entirely membrane-associated. To determine if ORP2 associates with detergent insoluble "raft" domains (25) in the CHO cell membranes, detergent lysates of the cells were analyzed in Optiprep™ step gradients in the presence of 1% Triton X-100 (26). Following centrifugation, all of the ORP2 species were quantitatively recovered in the detergent soluble "non-raft" fraction (data not shown).

The intracellular distribution of ORP2 in CHO cells was assessed by indirect immunofluorescence microscopy using the affinity-purified antibody (**Fig. 7**). In addition to a diffuse cytosolic aspect, a weak perinuclear staining of endogenous ORP2 was evident (Fig. 7A). The immunostaining was efficiently inhibited by preincubation of the antibody with the GST-ORP2 fusion protein (Fig. 7B), but not by incubation with GST (Fig. 7A). In stably transfected CHO cells overexpressing ORP2, a similar but markedly stronger staining was observed (Fig. 7C). The bright perinuclear aspect of this staining coincided with that of FITC-lentil lectin, a marker of the Golgi apparatus (Fig. 7D).

To determine if ORP2 plays a role in cellular cholesterol metabolism, we created a stably transfected CHO cell line (ORP2/CHO) that overexpresses ORP2 approximately 5-fold compared with the endogenous protein level. Mock-transfected and ORP2/CHO cells were labeled with [^{14}C]cholesterol for 36 h in culture medium containing 10% FBS, and efflux of radioactive cholesterol to human serum (20%), apoA-I (20 μg/ml), or to small unilamellar PC vesicles (0.3 mg PC/ml) was measured. In the experiments measuring apoA-I mediated efflux (27–29), BSA was used as a non-specific acceptor. During the 2 h efflux period of the [^{14}C]cholesterol to human serum, a significantly higher amount of the labeled cholesterol was transferred to the acceptor from the ORP2/CHO as compared with mock-transfected cells, the relative increment being approximately 40% (**Fig. 8A**). As for the serum acceptor, ORP2/CHO showed a marked increase in cholesterol delivery to apoA-I as compared with mock-transfected CHO, the relative difference being around 50% (Fig. 8B). A similar ORP2-induced cholesterol efflux increment was also detected when POPC vesicles were used as an acceptor (Fig. 8C).

The amount of cell-associated [^{14}C]cholesterol found in esterified form after the labeling period was determined by thin-layer chromatography. The proportion of the total [^{14}C]cholesterol found in the ester fraction was markedly reduced in the ORP2/CHO cells as compared with mock cells (**Fig. 9A**). The ORP2-induced efflux increment was thus associated with a 40–50% relative decrease in the [^{14}C]cholesteryl esters. To elucidate if this esterification defect reflected reduced ACAT activity in ORP2/CHO, we measured the [^{14}C]oleyl-CoA incorporation into CE by semipurified cellular membranes (Fig. 9B). This was done in the presence of exogenously added cholesterol to compensate for the difference observed in the cellular cholesterol levels (see below). The ACAT activity of ORP2/CHO was found to be reduced by ~45% as compared with the mock transfected cells.

To determine whether the ORP2-induced changes observed in the efflux and esterification of radioactive cholesterol reflect changes in the overall cellular cholesterol pools, we measured the cellular content of total choles-

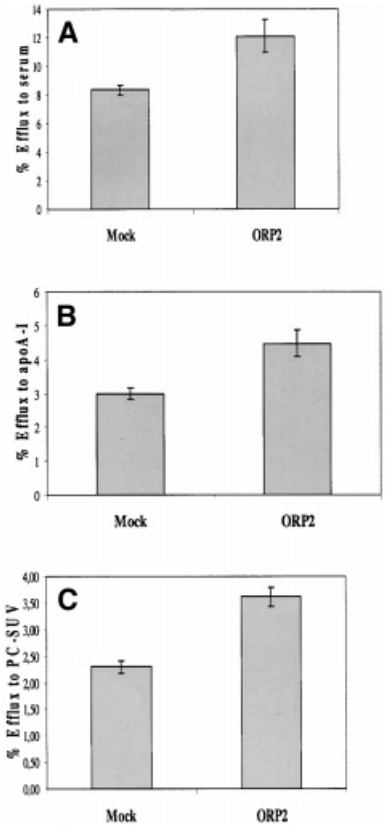

Fig. 8. The effect of ORP2 overexpression on [^{14}C]cholesterol efflux from CHO cells. Mock-transfected (Mock) or stably transfected ORP2 expressing CHO cells (ORP2) were labeled with [^{14}C]cholesterol for 36 h. They were then incubated with media containing different acceptors for cholesterol efflux. The radioactivity in the media and in the cells was determined by scintillation counting. A: Efflux (2 h) to 20% human serum. B: Efflux (4 h) to 20 μg/ml human apoA-I. Unspecific efflux to 0.2% BSA has been subtracted. C: Efflux (4 h) to small unilamellar palmitoyl-oleyl-PC vesicles (0.3 mg PC/ml). The results represent the percentage of total ^{14}C radioactivity found in the efflux medium. Representative experiments performed in triplicate (mean ± SEM) are shown.

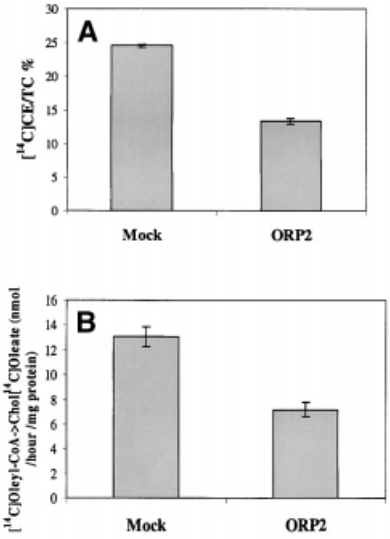

Fig. 9. The effect of ORP2 overexpression on cholesterol esterification in CHO cells. A: The proportion of the total cellular [^{14}C]cholesterol radioactivity recovered in the CE fraction was determined after the 36 h labeling period. B: The ACAT activity in cells cultured in serum-containing medium was assayed by measuring the rate of conversion of [1-^{14}C]oleyl-CoA to into cholesteryl [^{14}C]oleate by semipurified cellular membranes. Mock = mock-transfected CHO-K1 cells; ORP2 = ORP2 transfected CHO-K1 cell line. Representative experiments performed in triplicate (mean ± SEM) are shown.

terol (TC), free cholesterol (FC), and CE using enzymatic methods. For mock-transfected cells the values were TC, 34 μg/mg protein; FC, 26 μg/mg protein; and CE, 8.8 μg/mg protein, whereas the values for ORP2/CHO were 28 μg/mg protein, 23 μg/mg protein, and 5.1 μg/mg protein, respectively. These results suggest that under the cell culture conditions used, over expression of ORP2 causes a significant decrease in cellular TC (17%), FC (8.7%), and CE (42%), the relative decrease in CE being the most pronounced.

A yeast homolog of OSBP, Kes1p/Osh4p, is implicated in the Golgi apparatus secretory function (14). To test whether ORP2 overexpression has an effect on the biosynthetic pathway in CHO cells, we used a GFP-tagged vesicular stomatitis virus G (VSVG) protein as a marker. The VSVG carries a temperature-sensitive ts045 mutation causing its arrest in the endoplasmic reticulum (ER) at the restrictive temperature (40°C). The protein can be synchronously released from the ER by a shift to permissive temperature (32°C) (30). The cells transfected with a control plasmid pcDNA3.1/CAT or the ORP2 expression plasmid pcDNA3.1/ORP2 together with a VSVG3-GFP expression plasmid, were kept at 40°C for 20 h, and then shifted to 32°C for increasing time periods in the presence of cycloheximide to prevent further protein synthesis during the low temperature chase. In cells transfected with the control plasmid, VSVG-GFP was before chase exclusively associated with reticular ER structures (**Fig. 10A**). During 1 h of chase it was transported from the ER to the perinuclear Golgi apparatus (Fig. 10B), and by 4 h of chase practically all of the marker protein had reached the plasma membrane, with no significant staining detectable in the Golgi region (Fig. 10C). In cells overexpressing ORP2, the transport of VSVG-GFP proceeded in a similar fashion from the ER to the Golgi apparatus. However, after 4 h of chase a major portion of cells expressing ORP2 at high levels still displayed strong VSVG-GFP fluorescence in the Golgi region, in addition to plasma membrane fluorescence (Fig. 10D–I). The effect was not observed in cells expressing ORP2 at moderate levels such as those seen in the stably transfected cells used in the efflux studies. The results suggest that extensive overexpression of ORP2 interferes with the normal function of the late secretory pathway.

DISCUSSION

In the present study we report on characteristics of the recently identified OSBP-related protein ORP2. The protein lacks the *N*-terminal extension containing a PH domain present in the other OSBP protein family members (16). In this respect it resembles structurally the short (≈50 kDa) OSBP homologs of *S. cerevisiae*, Kes1p/Osh4p, Osh5p, Osh6p, and Osh7p (13). The amino acid sequence of ORP2, however, is most closely related to that of ORP1, a long PH-domain containing human protein (16). The ORP2 mRNA is expressed ubiquitously in mammalian tissues. The Western blot analysis of ORP2 protein in mouse tissues is consistent with the mRNA expression studies, demonstrating that the ORP2 protein is ubiquitously expressed but is most abundant in the brain. This suggests that ORP2 has an important housekeeping-type function, and it may be required in increased amounts in the nervous system, which constitutes the most cholesterol-rich tissues of our body.

In most of the mouse tissues analyzed, the ORP2 protein is detected as two major immunoreactive forms. Of these, the larger 56 kDa form is encoded by the cDNA used in this study. The smaller form most probably represents a variant translated from a differentially spliced version of the mRNA or a proteolytically processed product. The association of OSBP with the Golgi apparatus has been attributed to the PH domain in the *N*-terminal part of the protein, and it has been reported that binding of 25-OHC to the sterol binding domain of OSBP induces a shift of the protein from cytosol to Golgi membranes (8–10). Of the endogenous 56 and 51 kDa ORP2 proteins, a major portion is cytosolic but a portion of these proteins, as well as the overexpressed ORP2, apparently associates with membranes in the perinuclear region of CHO cells and colocalizes with a Golgi apparatus marker. Thus, ORP2 seems to be capable of Golgi association in the absence of a PH domain. The protein is obviously associated with membranes via other mechanisms, such as interaction of the ligand-binding domain with membrane lipids, or possibly through a ligand-induced conformational change exposing a yet unknown membrane interaction motif. The third 60 kDa form of ORP2 detected in CHO cells is fully

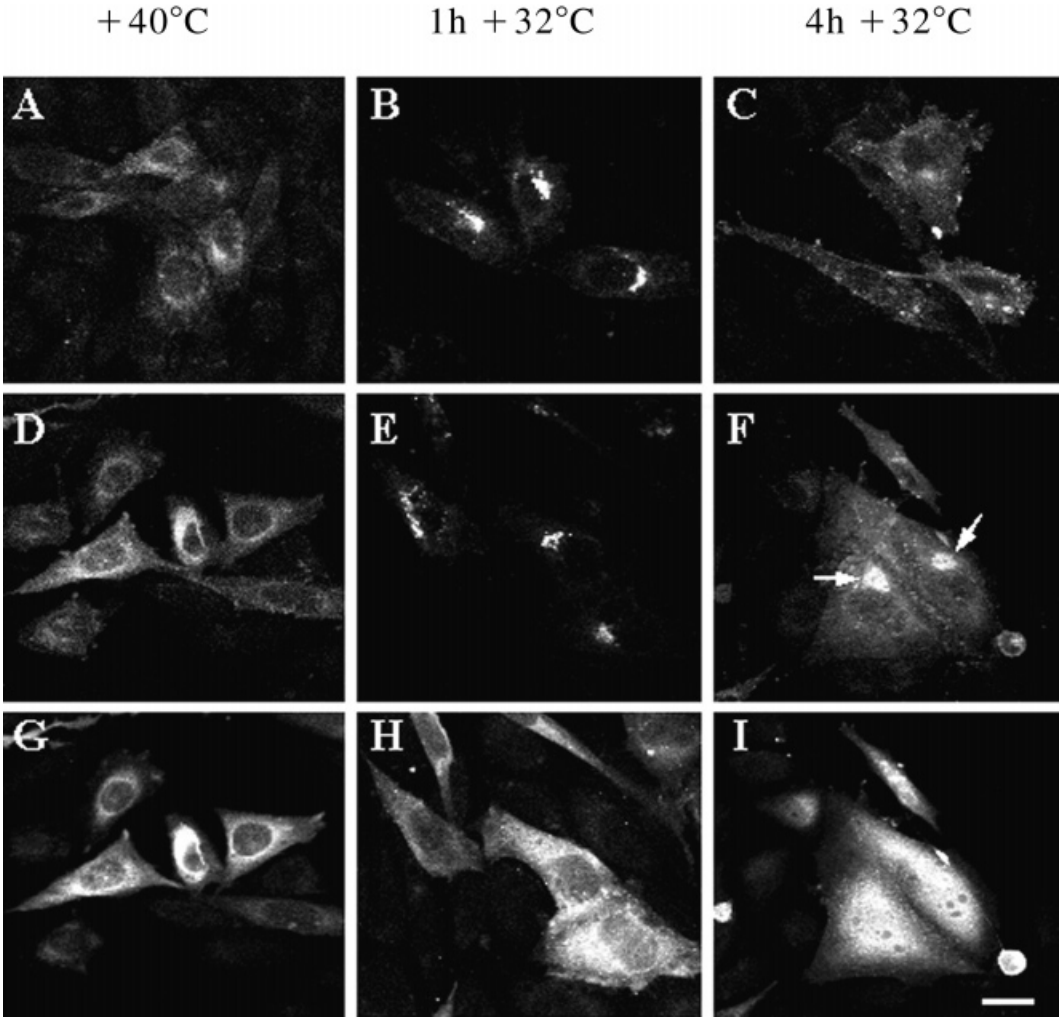

Fig. 10. The effect of ORP2 overexpression on protein trafficking along the secretory pathway. CHO cells were double transfected with a VSVG3-GFP expression plasmid and either pcDNA3.1/CAT (A–C) or pcDNA3.1/ORP2 (D–I). After incubation at 40°C (restrictive temperature), cycloheximide was added and the cells were shifted to 32°C (permissive temperature) for increasing time periods (indicated on the top). The cells were then fixed and GFP fluorescence was monitored under a confocal fluorescence microscope; ORP2 expression was visualized by indirect immunofluorescence staining. A, D, G, cells fixed directly at the end of the 40°C incubation; B, E, H, cells fixed after 1 h of chase at 32°C; C, F, I, cells fixed after 4 h of chase. A–F: VSVG-GFP fluorescence and panels G-I ORP2 immunostaining of the cells seen in D–F. The arrows in F indicate VSVG-GFP fluorescence remaining in the Golgi region after 4 h of chase. Bar = 10 μm.

membrane-bound. To elucidate the underlying mechanism molecular cloning of this isoform is required.

Xu et al. (31) recently reported that a variant of ORP2 lacking amino acid residues 13–24 does not bind 25-OHC. We have obtained similar results using a ligand-binding assay that employs His_6-tagged recombinant ORP2 protein (data not shown). Instead, Xu et al. found that ORP2 interacts with phosphatidic acid (PA), and weakly also with phosphatidyl inositol-3-phosphate. For a group of proteins carrying a StAR-type lipid binding domain, it has been shown that a similar binding domain can be used to accommodate very different types of lipid ligands, such as cholesterol in MNL64 and phosphatidyl choline in PC-transfer protein (32). Therefore, it is plausible also that ORP proteins could accommodate different types of lipids in their binding domain and thus participate in a spectrum of regulatory processes in cellular lipid metabolism.

Overexpression of ORP2 in stably transfected CHO cells resulted in a significant enhancement of [^{14}C]cholesterol efflux to all three acceptors used: serum, apoA-I, and PC vesicles. The enhancement of efflux was accompanied by a marked decrease in esterified [^{14}C]cholesterol and in ACAT activity. An effect of ORP2 was also evident when the TC, FC, and CE contents of the cells were determined. Expression of ORP2 caused a decrease in the cellular cholesterol levels, the effect being most prominent on the cellular CE content. In the light of these results it seems possible that downregulation of ACAT activity would represent a more direct effect of ORP2 overexpression, which would lead to increased availability of free [^{14}C]cholesterol for efflux. Consistent with our results, this should lead to an increase in both

apolipoprotein-mediated and diffusion-based removal of cellular cholesterol (27–29). The mechanisms by which an excess of ORP2 affects the esterification and efflux of cellular cholesterol are at present unknown. We observed no direct binding of cholesterol to ORP2 (data not shown). It is therefore unlikely that ORP2 would function as a cholesterol carrier or a factor that sequesters free cholesterol, but it may rather affect cellular cholesterol metabolism by some other, perhaps more indirect, mechanism.

Overexpression of ORP2 by transient plasmid transfection was found to interfere with the clearance of the GFP-tagged VSVG protein, a well-established marker of the secretory pathway trafficking, from the Golgi apparatus. The expression level of ORP2 in cells that displayed disturbance of VSVG transport was markedly higher (as judged by immunofluorescence microscopy) than that present in the stably transfected ORP2/CHO, in which cholesterol efflux and esterification were studied. Therefore, one cannot, based on our data, draw conclusions on the possible mechanistic connections of the two effects observed. The finding of ORP2-induced disturbance of VSVG transport is in line with results demonstrating that overexpression of an ORP2 variant in yeast cells perturbs the transport of carboxypeptidase Y to the yeast vacuole (31). Furthermore, the yeast OSBP homolog Kes1p/Osh4p has been suggested to negatively regulate the generation of secretory vesicles from the Golgi (14). The present data suggest that there might be functional similarities between ORP2 and yeast Kes1p/Osh4p. It is well established that phospholipase D, which cleaves PC to choline and PA, plays an important role in vesicular transport from the Golgi (33, 34). PA shows affinity for several components of the protein machinery of vesicle transport (35) and has been suggested to play an important role in transport vesicle formation (36–39). One can speculate that binding of excessive amounts of ORP2 to Golgi membrane PA may lead to displacement of vesicle transport machinery from the membranes and thus to a disturbance of vesicle formation.

The authors acknowledge Seija Puomilahti, Pirjo Ranta, and Ritva Keva for skilled technical assistance. Prof. Ingemar Björkhem (Karolinska Institute, Huddinge, Sweden) is thanked for kindly providing labeled oxysterols, Dr. Patrick Keller (Max-Planck Insitute of Molecular Cell Biology and Genetics, Dresden, Germany) for the VSVG3-GFP expression plasmid, Dr. Johan Peränen (Institute of Biotechnology, University of Helsinki, Finland) for the pGAT-4 vector, and Dr. T. Nagase (Kazusa DNA Research Institute, Chiba, Japan) for the KIAA0772 cDNA. This study was supported by the Finnish Cultural Foundation (S.L.), the Academy of Finland (grants 45817 and 50641 to V.M.O; 49987 and 43184 to E.I.; 68290 and 71234 to E.L.), and the Sigrid Juselius Foundation (V.M.O.).

Manuscript received 25 June 2001 and in revised form 19 October 2001.

REFERENCES

1. Russell, D. W. 2000. Oxysterol biosynthetic enzymes. *Biochim. Biophys. Acta.* **1529:** 126–135.
2. Bjorkhem, I., and G. Eggertsen. 2001. Genes involved in initial steps of bile acid synthesis. *Curr. Opin. Lipidol.* **12:** 97–103.
3. Brown, A. J., and W. Jessup. 1999. Oxysterols and atherosclerosis. *Atherosclerosis.* **142:** 1–28.
4. Schoonjans, K., C. Brendel, D. Mangelsdorf, and J. Auwerx. 2000. Sterols and gene expression: control of affluence. *Biochim. Biophys. Acta.* **1529:** 114–125.
5. Repa, J. J., and D. J. Mangelsdorf. 2000. The role of orphan nuclear receptors in the regulation of cholesterol homeostasis. *Annu. Rev. Cell. Dev. Biol.* **16:** 459–481.
6. Taylor, F. R., S. E. Saucier, E. P. Shown, E. J. Parish, and A. A. Kandutsch. 1984. Correlation between oxysterol binding to a cytosolic binding protein and potency in the repression of hydroxymethylglutaryl coenzyme A reductase. *J. Biol. Chem.* **259:** 12382–12387.
7. Taylor, F. R., and A. A. Kandutsch. 1985. Oxysterol binding protein. *Chem. Phys. Lipids.* **38:** 187–194.
8. Ridgway, N. D., P. A. Dawson, Y. K. Ho, M. S. Brown, and J. L. Goldstein. 1992. Translocation of oxysterol binding protein to golgi apparatus triggered by ligand binding. *J. Cell Biol.* **116:** 307–319.
9. Lagace, T. A., D. M. Byers, H. W. Cook, and N. D. Ridgway. 1997. Altered regulation of cholesterol and cholesteryl ester synthesis in Chinese-hamster ovary cells overexpressing the oxysterol-binding protein is dependent on the pleckstrin homology domain. *Biochem. J.* **326:** 205–213.
10. Levine, T. P., and S. Munro. 1998. The pleckstrin homology domain of oxysterol-binding protein recognises a determinant specific to Golgi membranes. *Curr. Biol.* **l8:** 729–739.
11. Brown, M. S., and J. L. Goldstein. 1999. A proteolytic pathway that controls the cholesterol content of membranes, cells, and blood. *Proc. Natl. Acad. Sci. USA.* **96:** 11041–11048.
12. Lagace, T. A., D. M. Byers, H. W. Cook, and N. D. Ridgway. 1999. Chinese hamster ovary cells overexpressing the oxysterol binding protein (OSBP) display enhanced synthesis of sphingomyelin in response to 25-hydroxycholesterol. *J. Lipid Res.* **40:** 109–116.
13. Beh, C. T., L. Cool, J. Phillips, and J. Rine. 2001. Overlapping functions of the yeast oxysterol-binding protein homologues. *Genetics.* **157:** 1117–1140.
14. Fang, M., B. G. Kearns, A. Gedvilaite, S. Kagiwada, M. Kearns, M. K. Fung, and Bankaitis V.A. 1996. Kes1p shares homology with human oxysterol binding protein and participates in a novel regulatory pathway for yeast Golgi-derived transport vesicle biogenesis. *EMBO J.* **15:** 6447–6459.
15. Laitinen, S., V. M. Olkkonen, C. Ehnholm, and E. Ikonen. 1999. Family of human oxysterol binding protein (OSBP) homologues: a novel member implicated in brain sterol metabolism. *J Lipid Res.* **40:** 2204–2211.
16. Lehto, M., S. Laitinen, G. Chinetti, M. Johansson, C. Ehnholm, B. Staels, E. Ikonen, and V. M. Olkkonen. 2001. The OSBP-related protein family in humans. *J. Lipid Res.* **42:** 1203–1213.
17. Musacchio, A., T. Gibson, P. Rice, J. Thompson, and M. Saraste. 1993. The PH domain: a common piece in the structural patchwork of signalling proteins. *Trends Biochem. Sci.* **18:** 343–348.
18. Nagase, T., K. Ishikawa, M. Suyama, R. Kikuno, N. Miyajima, A. Tanaka, H. Kotani, N. Nomura, and O. Ohard. 1998. Prediction of the coding sequences of unidentified human genes. XI. The complete sequences of 100 new cDNA clones from brain which code for large proteins in vitro. *DNA Res.* **5:** 277–286.
19. Lehtonen, S., V. M. Olkkonen, M. Stapleton, M. Zerial, and E. Lehtonen. 1998. HMG-17, a chromosomal non-histone protein, shows developmental regulation during organogenesis. *Int. J. Dev. Biol.* **42:** 775–782.
20. Toomre, D., P. Keller, J. White, J. C. Olivo, and K. Simons. 1999. Dual-color visualization of trans-Golgi network to plasma membrane traffic along microtubules in living cells. *J. Cell Sci.* **112:** 21–33.
21. Bligh, E. G., and W. J. Dyer. 1959. A rapid method of total lipid extraction and purification. *Can. J. Biochem. Physiol.* **37:** 911–917.
22. Heino, S., S. Lusa, P. Somerharju, C. Ehnholm, V. M. Olkkonen, and E. Ikonen. 2000. Dissecting the role of the golgi complex and lipid rafts in biosynthetic transport of cholesterol to the cell surface. *Proc. Natl. Acad. Sci. USA.* **97:** 8375–8380.
23. Johnson, W. J. 1996. Cell-free transfer of cholesterol from lysosomes to phospholipid vesicles. *J. Lipid Res.* **37:** 54–66.
24. Metherall, J. E., N. D. Ridgway, P. A. Dawson, J. L. Goldstein, and M. S. Brown. 1991. A 25-hydroxycholesterol-resistant cell line deficient in acyl-CoA:cholesterol acyltransferase. *J. Biol. Chem.* **266:** 12734–12740.

25. Simons, K., and E. Ikonen. 1997. Functional rafts in cell membranes. *Nature.* **387:** 569–572.
26. Harder, T., P. Scheiffele, P. Verkade, and K. Simons. 1998. Lipid domain structure of the plasma membrane revealed by patching of membrane components. *J. Cell Biol.* **141:** 929–942.
27. Rothblat, G. H., M. de la Llera-Moya, V. Atger, G. Kellner-Weibel, D. L. Williams, and M. C. Phillips. 1999. Cell cholesterol efflux: integration of old and new observations provides new insights. *J. Lipid Res.* **40:** 781–796.
28. Fielding, J. C., and P. E. Fielding. 2001. Cellular cholesterol efflux. *Biochim. Biophys. Acta.* **55822:** 1–15.
29. Yokoyama, S. 2001. Release of cellular cholesterol: molecular mechanism for cholesterol homeostasis in cells and in the body. *Biochim. Biophys. Acta.* **1529:** 231–244.
30. Lippincott-Schwartz, J., T. H. Roberts, and K. Hirschberg. 2000. Secretory protein trafficking and organelle dynamics in living cells. *Annu. Rev. Cell Dev. Biol.* **16:** 557–589.
31. Xu, Y., Y. Liu, N. D. Ridgway, and C. R. McMaster. 2001. Novel members of the human oxysterol-binding protein family bind phospholipids and regulate vesicle transport. *J. Biol. Chem.* **276:** 18407–18414.
32. Tsujishita, Y., and J. H. Hurley. 2000. Structure and lipid transport mechanism of a StAR-related domain. *Nat. Struct. Biol.* **7:** 408–414.
33. Ktistakis, N. T. 1998. Signaling molecules and regulation of intracellular transport. *BioEssays.* **20:** 495–502.
34. Roth, M. G. 1999. Lipid regulators of membrane traffic through the Golgi complex. *Trends Cell. Biol.* **9:** 174–179.
35. Manifava, M., J. W. Thuring, Z. Y. Lim, L. Packman, A. B. Holmes, and N. T. Ktistakis. 2001. Differential binding of traffic-related proteins to phosphatidic acid- or phosphatidylinositol (4,5)-bisphosphate-coupled affinity reagents. *J. Biol. Chem.* **276:** 8987–8994.
36. Matsuoka, K., L. Orci, M. Amherdt, S. Y. Bednarek, S. Hamamoto, R. Schekman, and T. Yeung. 1998. COPII-coated vesicle formation reconstituted with purified coat proteins and chemically defined liposomes. *Cell.* **93:** 263–275.
37. Takei, K., V. Haucke, V. Slepnev, K. Farsad, M. Salazar, H. Chen, P. De Camilli. 1998. Generation of coated intermediates of clathrin-mediated endocytosis on protein-free liposomes. *Cell.* **94:** 131–141.
38. Weigert, R., M. G. Silletta, S. Spano, G. Turacchio, C. Cericola, A. Colanzi, S. Senatore, R. Mancini, E. V. Polishchuk, M. Salmona, F. Facchiano, K. N. Burger, A. Mironov, A. Luini, and D. Corda. 1999. CtBP/BARS induces fission of Golgi membranes by acylating lysophosphatidic acid. *Nature.* **402:** 429–433.
39. Schmidt, A., M. Wolde, C. Thiele, W. Fest, H. Kratzin, A. V. Podtelejnikov, W. Witke, W. B. Huttner, and H. D. Soling. 1999. Endophilin I mediates synaptic vesicle formation by transfer of arachidonate to lysophosphatidic acid. *Nature.* **401:** 133–141.